Universitat Politècnica de Catalunya (UPC)
Universitat Autònoma de Barcelona (UAB)
Universitat de Barcelona (UB)
Institut de Ciències Fotòniques (ICFO)

http://www.photonicsbcn.eu

Master in Photonics

MASTER THESIS WORK

ANGULAR RADIATION PATTERNS OF NANOANTENNAS: AN OPTICAL YAGI-UDA ANTENNA

Alberto González Curto

Supervised by Prof. Niek van Hulst, (ICFO)

Presented on date 9th September 2009

Registered at

Escola Tècnica Superior d'Enginyeria de Telecomunicació de Barcelona

Angular Radiation Patterns of Nanoantennas: an Optical Yagi-Uda Antenna

Alberto González Curto

ICFO-Institut de Ciencies Fotoniques, Mediterranean Technology Park, 08860 Castelldefels (Barcelona), Spain

E-mail: alberto.curto@icfo.es

Abstract. We address experimentally the radiation patterns of quantum dots coupled to optical nanoantennas at specific positions. We show that the emission of the coupled system is determined by a variety of resonant and non-resonant antenna modes both in polarization and angular pattern. The first working optical Yagi-Uda antenna is presented and unidirectional emission is demonstrated for a limited spectral bandwidth. Our results show that the Yagi-Uda radiative efficiency is comparable to that of a half-wave dipole antenna.

Keywords: Nanophotonics, Optical antennas, Quantum dots, Scattering

1. Introduction

Optical antennas are the visible counterparts of conventional radio frequency and microwave antennas for frequencies in the visible regime (~ 500 THz) [1,2]. They localize optical fields to sub-diffraction-limited volumes, enhance and redirect the excitation and emission of quantum emitters as well as modify their spectra. They open up exciting opportunities in fields ranging from nonlinear light-matter interaction to superresolution microscopy [3–6]. In the nanometer scale, diffraction poses a limit to the collimated beaming of light. One of the most remarkable and recognizable characteristics of antennas is directed emission or reception. Although the control of directionality by photonic crystal structures [7, 8] and surface-plasmon-based devices [9, 10] has been studied, plasmonic nanoantennas offer intrinsic additional advantages such as a much smaller footprint, strong electromagnetic field enhancement and suitability for single-molecule studies.

Modification of the angular emission of molecules by objects in their near field has been reported in the literature in recent years [11–13]. Several authors have made theoretical studies aiming for unidirectional emission of optical dipoles [14–17] but the goal has remained elusive in practice. In particular, optical Yagi-Uda (YU) antennas bring this effect to the nanoscale together with increased transition rates. More specifically, the YU design consists of an active or driving element (feed) and a number of

parasitic elements acting as reflectors and directors that are longer or shorter compared to the feed, respectively. As a result, its radiation points towards the directors. In the optical domain, it has been proposed to substitute the feed element by a point source. A molecule, for instance, would be surrounded by a set of core-shell nanoparticles [14] or metal nanorods [15]. Our approach includes the feed element [16], which is driven locally by an optical source, thus preserving the local field enhancement. We also apply the same strategy to evaluate the angular radiation patterns of non-dipolar [18,19] antennas obtaining signatures of several high-order modes and providing qualitative explanations of our observations.

In the first section of this thesis, we set out the basic concepts about antenna theory that will help us to understand the results. Next, the experimental methods of fabrication and measurement are explained. The results section begins with an evaluation of radiation patterns of bare molecules and quantum dots. Then, we show the angular patterns of nanowire antennas and proceed to demonstrate the first experimental realization of directed emission by an optical YU antenna. We finish with some suggestions of further research directions and possible applications of our work.

2. Coupling of emitters to an optical antenna

Feeding energy into an optical antenna is a task that can be accomplished from the far field (i.e. scattering) [20] or from the near field by a local optical emitter. We choose the latter option because it offers the possibility of exciting a nanostructure at designated positions as opposed to driving the whole nanostructure simultaneously. There are two ways of driving the antenna modes from its near field: either by local deposition of emitters (static) or by scanning the antenna over the emitter or vice versa (dynamic). In the present work, we opt for the static approach and locally deposit semiconductor nanocrystals selectively on nanoantennnas.

For small nanoparticles, the interaction of a point source with a nanorod can be regarded as a dipole-dipole interaction where the nanorod is dominant. This holds true at least until the first resonance is reached at half of the effective wavelength in the metal rod [21]. Interaction with longer nanorods can be understood in terms of plasmon standing waves excited by an incident electric field. Under such a model, the resonances are found at integer multiples j of half the effective wavelength $L_j = j\lambda_{eff}/2$, with λ_{eff} depending on material and geometrical parameters. Hence, multipole resonances are modes with more than one intensity node along a one-dimensional resonator and any resonant mode will couple to an emitter efficiently from the ends, where the density of electromagnetic modes is higher. The strength of this coupling can lead to a complete modification of the polarization or angular pattern [12, 22]. In general, direct angular detection is preferred as polarization measurements do not give access to all the available information (e.g. asymmetric radiation patterns).

3. Experimental methods

3.1. Fabrication

Positioning a single emitter with respect to a nanostructure in a permanent fashion constitutes a formidable nanotechnological challenge. We rely on a two-step electron beam lithography technique combined with chemical functionalization to deposit patches of colloidal quantum dots (QD) at designated locations. We employ polymethyl methacrylate (PMMA) as a positive electronic resist. The substrates are made of glass and have a layer of 10 nm of indium tin oxide (ITO). The fabrication process is divided in three parts: an initial lithography to fabricate the metal nanostructures is followed, after thermal evaporation of a 30-nm layer of Au, by a second lithography to define the positions of the QDs and, thirdly, by the deposition of the QDs. The final layout is depicted in Fig. 1(c). We employ water-soluble, core-shell quantum dots with a polymer coating (Invitrogen, Qdot 800 ITK amino (PEG)). Their emission is centered around 790 nm with a full width at half maximum of 85 nm. We use QDs instead of fluorescent molecules due to their higher resistance to photobleaching, good quantum efficiencies and broader excitation spectrum.The wavelength choice was guided by material parameters and fabrication capabilities. In order to bind the QDs to one part of the Au nanoantennas and not to the rest of the substrate, we functionalize the Au surface exclusively inside the PMMA gaps produced by the second lithography. A self-assembled monolayer of mercaptoundecanoic acid (MUA) is formed in the areas exposed to the e-beam as it adsorbs on the Au surface via its thiol groups. Next, a carbodiimide (EDC) activates the carboxylic acid terminations of MUA so that the amino groups of the QDs can bind to them. Finally, once the QDs are immobilized, the remaining PMMA is lifted off by rinsing in acetone. We achieve an accuracy of around 40 nm in positioning a QD patch relative to a metal structure. That is also the size of the smallest achievable patch.

3.2. Characterization

Our set-up is based on a Zeiss Axiovert 200 microscope with sample scanning and consists of two detection branches (see Fig. 1 (b)). The first one (right) is a confocal fluorescence microscope with single-emitter detection capabilities. The use of two avalanche photodiodes (APDs 1 & 2, Perkin Elmer, SPCM-AQR-14 and 16) allows us to detect polarization anisotropies thanks to a polarizing beamsplitter cube. The detectors themselves serve as confocal apertures. We make use of an oil immersion objective (Zeiss, α Plan-Apochromat 100x/1.46 NA). A collimated He-Ne laser beam (λ=633 nm) reflects on a long-pass dichroic mirror (Semrock, FF735-Di01) and a power on the order of μW reaches the focus exciting the QDs. The resulting luminescence from the sample passes through a long-pass filter (Omega Optical, 740 AELP) that further

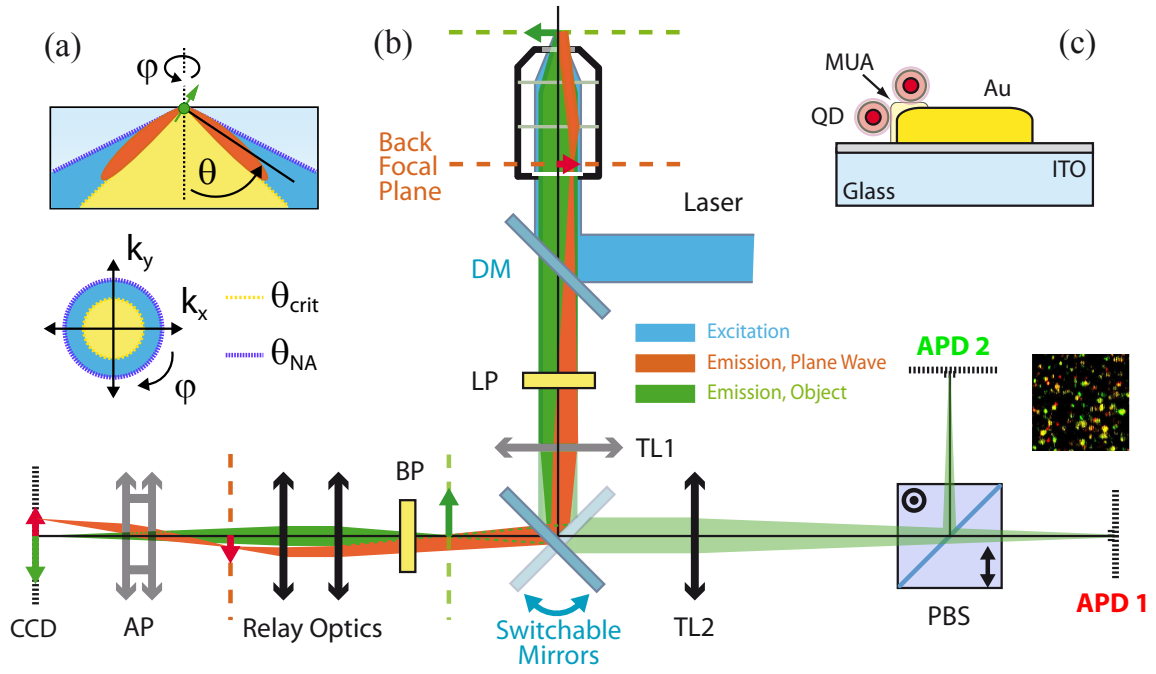

Figure 1. (a) Radiation pattern of a dipole close to a dielectric interface and explanation of angular imaging highlighting the critical and numerical aperture angles. (b) Set-up. DM: dichroic mirror; LP: long-pass filter; BP: band-pass filter; TL: tube lens; AP: achromat pair; PBS: polarizing beamsplitter; APD: avalanche photodiode. There are different configurations depending on the position of TL1 (in: conoscope; out: confocal) and AP (in: Fourier image; out: widefield image). The inset at the bottom corner shows a typical confocal image of single emitters. (c) Layout of a sample.

separates the excitation wavelength from the emission. When necessary, a band-pass filter (Thorlabs, FB800-10) around the emission peak of our QDs was utilised to narrow the detected bandwidth. The second part (left) of our set-up is devoted to angular detection and is referred to as a conoscope. It can record an image of the back focal plane of the objective, which contains the directions of emission, or alternatively a widefield image. Starting from the intermediate image of an object after the mirror (green), relay optics project the real space image onto a Peltier-cooled, back-illuminated CCD camera (Andor, DV 437-BV). At the same time, the relay optics form an intermediate image of the Fourier plane (red). Lastly, an achromat pair, that can be flipped in and out of the optical path, images the aforementioned plane onto the CCD chip. The signal is recorded during 49 seconds in 7 accumulation steps and is distributed over approximately 150x150 pixels. Diffraction gratings were used to calibrate the k-space images. The intensity content of the back focal plane of the objective is related to the angular pattern by a projection: $R(pixel) = K \sin\theta$, where θ is the inclination angle between the optical axis and the wavevector and K is a calibration constant.

4. Results

4.1. Emitters without nanostructures

As a reference, we assess first the characteristics of several kinds of emitters in the absence of antenna structures. Figure 2 shows the radiation patterns of a 200-nm fluorescent bead, a single molecule in a thin PMMA film, an ensemble of quantum dots and a single quantum dot embedded in PMMA. In all the four cases, the illumination was linearly polarized in the direction indicated by the arrow. First of all, in these k-space images we can observe two distinct circles: the outer one is the maximum collection angle of our objective ($\theta_{NA} = 72.8°$) and the inner one is the critical angle of a glass-air interface ($\theta_{crit} = 41.1°$). The effect of the substrate is to bend the donut-shaped pattern of a dipole towards the glass side peaking at the critical angle, as explained in Fig. 1(a). The emission from an ensemble of randomly oriented molecules inside

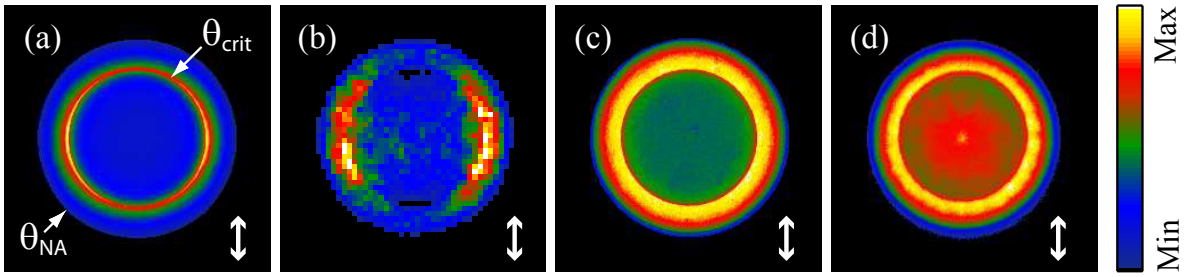

Figure 2. Radiation patterns of the emission of several types of emitters. (a) A polystyrene bead filled with fluorescent molecules, (b) a single molecule in a thin PMMA film, (c) an ensemble of quantum dots and (d) a single quantum dot in PMMA. The substrate is glass and the arrow indicates the direction of linear polarization of excitation. The single-molecule image (b) is binned 4 times in order to compensate for a dimmer signal.

a bead is dominated by dipoles oriented parallel to the incident polarization. Note that the directions of emission are perpendicular to the direction of oscillation (arrow) and most of the radiation is contained between the critical angle and the maximum collection angle. The case of a single molecule is similar but the pattern is that of a single dipole [23], that is to say the characteristic double-lobe pattern. By way of contrast, quantum dots are known to exhibit degenerate transition dipole moments oriented isotropically in two dimensions [24–27]. This fact depends on the crystalline structure of the nanoscrystal and implies that a QD can be excited and emit with a polarization that lies on a "bright" plane, as opposed to a molecular linear dipole with a "bright" axis. Effectively, this means that the luminescence of QDs has components deviating from the incident polarization. This is demonstrated by comparison of figures (a) and (b) with (c) and (d) in Fig. 2. Consequently, the angular pattern of a QD resembles a more uniform ring shape.

4.2. Nanowire antennas

Based upon full 3D numerical simulations (CST, Microwave Studio), we identified the resonant lengths of a nanorod for a dipole emitting at λ=800 nm in the near field. The

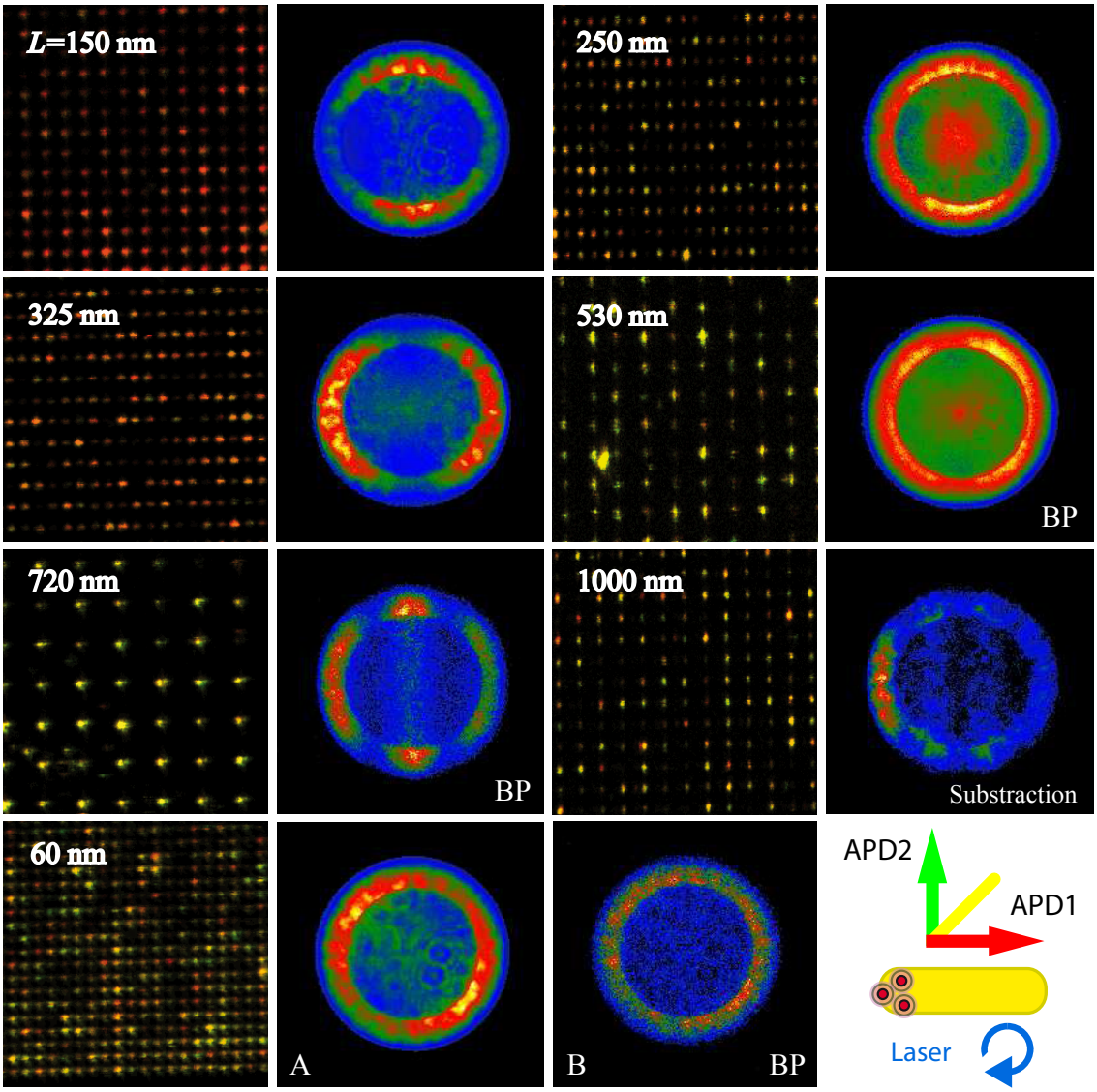

Figure 3. Nanowire antennas of increasing length L. Pairs of confocal luminescence images and k-space images corresponding to the length L indicated in white. Images labeled with BP where recorded using a band-pass filter around the emission maximum. The image tagged with substraction was obtained after numerical substraction of a ring. A and B belong to two different 60 nm squares. The intensity scale in conoscopic images goes from minimum to maximum. Confocal images show an area of 20x20 μm. In the bottom right corner, the orientation of the antennas is shown as well as the colour code for both polarization channels.

height of the nanowires is 30 nm and the width is 65 nm, which yielded the following resonant lengths in calculations: L=177 (j=1), 339 (j=2), 531 (j=3), 723 (j=4), 914 (j=5) and 1106 nm (j=6). Note that these calculations do not include the conductive ITO layer. Due to symmetry considerations, we expect that the radiation pattern of a nanowire possesses a central vertical stripe that is dark for an even mode and bright for an odd one.

In Fig. 3, we show pairs of confocal luminescence images of a matrix of antennas with a 100-nm patch of quantum dots at one end and a representative radiation pattern. The confocal images are colour coded (red/green) to visualize the degree of linear polarization. Here red corresponds to polarization along the axis of the nanowire. Illumination was circularly polarized for maximum efficiency in excitation. Noteworthily, the bidimensional transition moment of a QD can be converted into an effective linear dipole as can be noticed in the uniform red colour of Fig. 3 for L=150 and 325 nm. We identify these two cases with the half-lambda (j=1) and lambda (j=2) resonances. Note that the mode j=2 cannot be excited from the far field because it has no net dipole moment. Therefore, it is called a dark mode and can only be excited by near-field coupling of an emitter. The intermediate value L=250 nm lies between j=1 and j=2. It is partly polarized and its radiation pattern is similar to a half-wave dipole. The length L=530 nm, albeit identified as a resonance in the preliminary calculations (j=3), does not display polarization and we can barely distinguish a central minimum and four lobes in its pattern. If we increase the length of the bar to L=720 nm, the angular image shows a central bright band with two side lobes. This corresponds to an odd mode while simulations predicted it to be j=4. For the longest bar of the set (L=1000 nm), results were not conclusive but substraction of a ring pattern (radiation not coupled to the nanowire) leads us to a possible higher-order even mode. Furthermore, as a control matrix, we fabricated 60-nm Au squares. Its confocal image shows that the emission is not preferentially polarized as expected for a deeply subwavelength particle. For them, there are two types of radiation patterns. The first one (A) is reminescent of a dipole with random orientation, although there were more occurrences with orientation along the diagonal of the squares, as shown in the last line of Fig. 3. The second type (B) is similar to the ring pattern characteristic of QDs. In the presented sequence of nanowires, we can easily identify the appearance of new lobes as the length of the nanowires increases. We can also observe in our measurements that the patterns evolve alternating brighter or darker bands at the center which is consistent with increasing the resonance order from odd to even and so on. Unfortunately, towards longer nanowire theory and experiment start to deviate, which requires further study.

4.3. Yagi-Uda antennas

We fabricated 5-element YU antennas with a patch of QDs at one end of the feed element. The dimensions of each element were tuned in numerical calculations and subsequently fabricated (Fig. 4(a) and (d)). Note that compared to photonic crystals a YU antenna occupies even less than a typical unit cell. First of all, emission is clearly

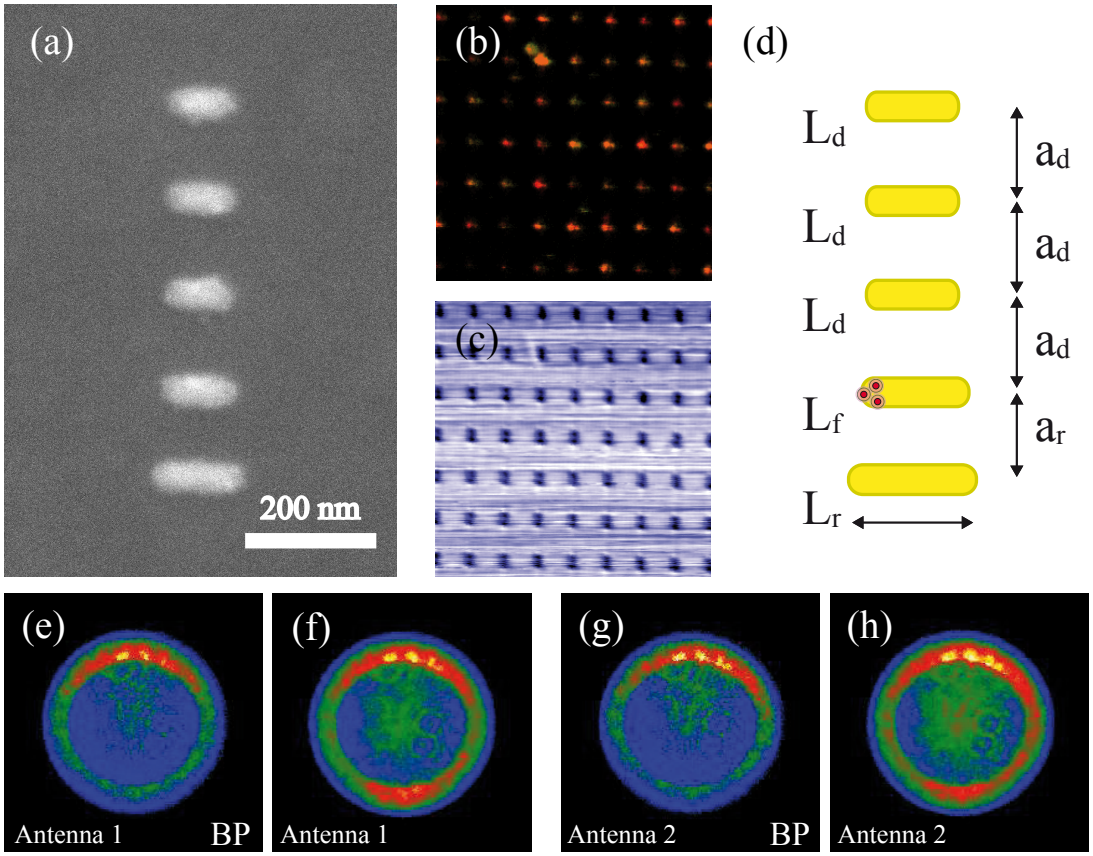

Figure 4. Optical Yagi-Uda antennas. (a) Scanning electron microscope image of a YU. (b) Confocal luminescence image (c) Transmission image recorded pixel by pixel by a photodiode above the sample. (d) Schematic of the design, where W=65, H=30, L_f=145, L_d=130, L_r=180, a_d=200 and a_r=180 nm. (e)-(h) Angular radiation patterns of two different YU antennas (e, f and g, h) with and without a band-pass filter (BP) respectively. The intensity scale in conoscopic images goes from minimum to maximum. Confocal and transmission images show an area of 20x20 μm.

polarized along the axis of the dipolar feed element as can be seen in Fig. 4(b). Adding a band-pass filter, we can recognize the end-fire operation of a YU in the upper, single lobe instead of the dipolar pattern with two lobes from the feed element alone (cf. figures 3 (L=150 nm right) and 4(e)). Conoscopic images without filter are shown for completeness where we can observe a lower lobe consisting of detuned frequencies. As in radio frequency YU antennas, the bandwidth is rather limited, between 10 and 85 nm.

A possible solution to increase the working wavelength range is to use a log-periodic antenna design [2]. The intensity detected from a YU is comparable but slightly smaller than that for the dipolar antennas shown in figure 3(a) suggesting that the radiation efficiencies have the same order of magnitude but suffer from extra parasitic losses in a multielement antenna. A complete characterization of all the structures will include measurements of luminescence lifetime and spectra for each kind of antenna. Finally, we emphasize that we have investigated mainly standing wave (resonant) antennas but traveling waves can also give rise to directionality. A popular example is a Beverage antenna [2], a long wire terminated in a matched load.

5. Conclusions

This thesis presents the first experimental realization of an optical Yagi-Uda antenna along with demonstration of multipolar radiation patterns from quantum dots coupled to nanowire antennas. The combination of our design, fabrication and experimental methods have proved to be a powerful technique that allows us to compare the angular emission of any kind of nanoemitter and control it. The assembly approach introduced here is particularly suitable for sensing applications as YU antennas offer a flat and compact platform, ready-to-use with any fluorophore that can be chemically attached to gold. Our antennas enable efficient detection of single emitters reducing the effective numerical aperture needed to collect their radiation and offering potential to increase their transition rates. Finally, we have only studied the modification of emission but optical antennas offer innovative ways of communication to, from and between quantum emitters.

Acknowledgments

The author acknowledges his Thesis Advisor Prof. Niek van Hulst as well as the people who contributed to this project: Giorgio Volpe, Tim Taminiau, Mark Kreuzer, Marta Castro and Romain Quidant. He also thanks all the members of the Molecular Nanophotonics group at ICFO for advice and helpful discussions.

References

[1] Bharadwaj P, Deutsch B and Novotny L 2009 Optical antennas *Adv. Opt. Photonics* **1** 438–483.
[2] Balanis C A 2005 *Antenna Theory: Analysis and Design* (New York: Wiley-Interscience).
[3] Mühlschlegel P, Eisler H J, Martin O J F, Hecht B and Pohl D W 2005 Resonant optical antennas *Science* **308** 1607.
[4] Farahani J N, Pohl D W, Eisler H J and Hecht B 2005 Single quantum dot coupled to a scanning optical antenna: a tunable superemitter *Phys. Rev. Lett.* **95** 017402.
[5] Kühn S, Hakanson U, Rogobete L and Sandoghdar V 2006 Enhancement of single-molecule fluorescence using a gold nanoparticle as an optical nanoantenna *Phys. Rev. Lett.* **97** 017402.

[6] Taminiau T H, Moerland R J, Segerink F B, Kuipers L and Hulst N F 2007 $\lambda/4$ resonance of an optical monopole antenna probed by single molecule fluorescence *Nano Lett.* **7** 28–33.
[7] Kramper P, Agio M, Soukoulis C M, Birner A, Muller F, Wehrspohn R B, Gosele U and Sandoghdar V 2004 Highly directional emission from photonic crystal waveguides of subwavelength width *Phys. Rev. Lett.* **92** 113903.
[8] Barth M, Schuster R, Gruber A and Cichos F 2006 Imaging single quantum dots in three-dimensional photonic crystals *Phys. Rev. Lett.* **96** 243902.
[9] Yu N, Fan J, Wang Q J, Pfluegl C, Diehl L, Edamura T, Yamanishi M, Kan H and Capasso F 2008 Small-divergence semiconductor lasers by plasmonic collimation *Nat. Photonics* **2** 564-570.
[10] Lezec H J, Degiron A, Devaux E, Linke R A, Martín-Moreno L, García-Vidal F J and Ebbesen T W 2002 Beaming light from a subwavelength aperture *Science* **297** 820–822.
[11] Gersen H, García-Parajó M F, Novotny L, Veerman J A, Kuipers L and van Hulst N F 2000 Influencing the angular emission of a single molecule *Phys. Rev. Lett.* **85** 5312.
[12] Taminiau T H, Stefani F D, Segerink F B and Van Hulst N F 2008 Optical antennas direct single-molecule emission *Nat. Photonics* **2** 234-237.
[13] Kühn S, Mori G, Agio M and Sandoghdar V 2008 Modification of single molecule fluorescence close to a nanostructure: radiation pattern, spontaneous emission and quenching *Mol. Phys.* **106** 893–908.
[14] Li J, Salandrino A and Engheta N 2007 Shaping light beams in the nanometer scale: A Yagi-Uda nanoantenna in the optical domain *Phys. Rev. B* **76** 245403.
[15] Hofmann H F, Kosako T and Kadoya Y 2007 Design parameters for a nano-optical Yagi-Uda antenna *New J. Phys.* **9** 217.
[16] Taminiau T H, Stefani F D and van Hulst N F 2008 Enhanced directional excitation and emission of single emitters by a nano-optical Yagi-Uda antenna *Opt. Express* **16** 10858–10866.
[17] Pakizeh T and Käll M 2009 Unidirectional Ultracompact Optical Nanoantennas *Nano Lett.* **9** 2343.
[18] Sharma N L 2007 Nondipole optical scattering from liquids and nanoparticles *Phys. Rev. Lett.* **98** 217402.
[19] Encina E R and Coronado E A 2008 Plasmonic Nanoantennas: Angular Scattering Properties of Multipole Resonances in Noble Metal Nanorods *J. Phys. Chem. C* **112** 9586-9594.
[20] Huang C, Bouhelier A, des Francs G C, Bruyant A, Guenot A, Finot E, Weeber J C and Dereux A 2008 Gain, detuning, and radiation patterns of nanoparticle optical antennas *Phys. Rev. B* **78** 155407.
[21] Novotny L 2007 Effective wavelength scaling for optical antennas *Phys. Rev. Lett.* **98** 266802.
[22] Shegai T, Li Z, Dadosh T, Zhang Z, Xu H and Haran G 2008 Managing light polarization via plasmon-molecule interactions within an asymmetric metal nanoparticle trimer *P. Natl. Acad. Sci. USA* **105** 16448-16453.
[23] Lieb M A, Zavislan J M and Novotny L 2004 Single-molecule orientations determined by direct emission pattern imaging *J. Opt. Soc. Am. B* **21** 1210-1215.
[24] Empedocles S A, Neuhauser R and Bawendi M G 1999 Three-dimensional orientation measurements of symmetric single chromophores using polarization microscopy *Nature* **399** 126.
[25] Koberling F, Kolb U, Potapova I, Phillip G, Basché T and Mews A 2003 Fluorescence anisotropy and crystal structure of individual semiconductor nanocrystals *J. Phys. Chem. B* **107** 7463–7471.
[26] Brokmann X, Coolen L, Hermier J and Dahan M 2005 Emission properties of single CdSe/ZnS quantum dots close to a dielectric interface *Chem. Phys.* **318** 91-98.
[27] Early K T, McCarthy K D, Odoi M Y, Sudeep P K, Emrick T and Barnes M D 2009 Linear dipole behavior in single CdSe-Oligo(phenylene vinylene) nanostructures *ACS Nano* **3** 453-461.